The EMBO Journal Vol.16 No.21 pp.6574–6583, 1997

DnaA protein binding to individual DnaA boxes in the *Escherichia coli* replication origin, *oriC*

Christoph Weigel, Andrea Schmidt, Beate Rückert, Rudi Lurz and Walter Messer[1]

Max-Planck-Institut für molekulare Genetik, Ihnestrasse 73, D-14195 Berlin-Dahlem, Germany

[1]Corresponding author
e-mail: messer@mpimg-berlin-dahlem.mpg.de

The formation of nucleoprotein complexes between the *Escherichia coli* initiator protein DnaA and the replication origin *oriC* was analysed *in vitro* by band-shift assays and electron microscopy. DnaA protein binds equally well to linear and supercoiled *oriC* substrates as revealed by analysis of the binding preference to individual DnaA boxes (9-mer repeats) in *oriC*, and by a competition band-shift assay. DnaA box R4 (*oriC* positions 260–268) binds DnaA preferentially and in the *oriC* context with higher affinity than expected from its binding constant. This effect depends on *oriC* positions 249 to 274, is enhanced by the wild-type sequence in the DnaA box R3 region, but is not dependent on Dam methylation or the curved DNA segment to the right of *oriC*. DnaA binds randomly to the DnaA boxes R1, M, R2 and R3 in *oriC* with no apparent cooperativity: the binding preference of DnaA to these sites was not altered for templates with mutated DnaA box R4. In the *oriC* context, DnaA box R1 binds DnaA with lower affinity than expected from its binding constant, i.e. the affinity is reduced to approximately that of DnaA box R2. Higher protein concentrations were required to observe binding to DnaA box M, making this low-affinity site a novel candidate for a regulatory DnaA box.

Keywords: band-shift assay/DnaA/electron microscopy/initiation complex/*oriC*

Introduction

Initiation of DNA replication requires the interaction of protein(s) with DNA, distorting the latter such that the localized disruption of base pairs exposes a single-strand template for the establishment of replication forks. Our model system is the interaction of DnaA, the initiator protein of *Escherichia coli*, with the chromosomal replication origin, *oriC* (Skarstad and Boye, 1994; Messer and Weigel, 1996).

Initiation of replication in *E.coli* proceeds through a series of biochemically defined stages (Kornberg and Baker, 1992). The first stage is the tight binding of several DnaA monomers to a supercoiled and fully *dam*-methylated *oriC* (260 bp) substrate, resulting in an initial complex (Fuller *et al.*, 1984; Funnell *et al.*, 1987; Crooke *et al.*, 1993; Woelker and Messer, 1993). This DnaA–*oriC* interaction is responsible for a local unwinding in the AT-rich region in the left part of *oriC*, the transition from initial to open complex (Bramhill and Kornberg, 1988; Gille and Messer, 1991; Hwang and Kornberg, 1992). Loading of the DnaBC helicase to the unwound region by an interaction between DnaA and DnaBC results in the pre-priming complex (Baker *et al.*, 1987; Sekimizu *et al.*, 1988a; Marszalek and Kaguni, 1994). Addition of SSB, DNA gyrase and DnaG primase leads to DnaA-mediated priming at start sites for bidirectional DNA synthesis in the right half of *oriC* (Seufert and Messer, 1987).

DnaA protein binds to five 9 bp consensus binding sites in *oriC*, called DnaA boxes (Fuller *et al.*, 1984; Matsui *et al.*, 1985) (see Table I and Figure 5). The importance of every single DnaA box [called R1, M, R2, R3 and R4 in the following (Messer and Weigel, 1996)] for normal *oriC* functioning *in vivo* was demonstrated in a recent study (Langer *et al.*, 1996). Analysis by electron microscopy revealed that DnaA–*oriC* nucleoprotein complexes are rather bulky, vary considerably in size and shape, with a fraction of those complexes containing 20–40 DnaA monomers being capable of open complex formation (Funnell *et al.*, 1987; Crooke *et al.*, 1993). Whether this reflects experimental limitations to determine the exact DnaA/*oriC* stoichiometry of the initial complex, or whether the transition from initial to open complex simply requires a certain threshold level of DnaA/*oriC*, remains to be established. Also, virtually nothing is known about specific DnaA–DnaA oligomerization at *oriC*.

DnaA protein binds to DNA by its C-terminal domain (domain 4) (Roth and Messer, 1995), and as a monomer *in vitro* (Schaper and Messer, 1995). Originally defined by DNase I footprint analysis (Fuller *et al.*, 1984; Matsui *et al.*, 1985; Yoshikawa and Ogasawara, 1991; Zakrzewska-Czerwinska and Schrempf, 1992), a more precise definition of the DnaA box as the site for specific DnaA binding came from the determination of binding constants: 5′-TT$^{A}/_{T}$TNCACA (Schaper and Messer, 1995). R1, R2 and R4, but not R3 and M, fulfil the sequence requirements of this stringent definition. The binding affinities vary by more than one order of magnitude among the individual motifs and depend also on the flanking sequences (Schaper and Messer, 1995). The DnaA box sequences, the distances between them and the orientation with respect to each other, can be manipulated to some extent without loss of *oriC* function. *oriC* mutants with an insertion or deletion of 10 bp (one helical turn) between R2 and R3, or R3 and R4 give functional origins (Messer *et al.*, 1992; Woelker and Messer, 1993). R2, R3 and R4, but not R1 and M, can be inverted without complete loss of *oriC* function (Langer *et al.*, 1996). These findings suggest that the positioning of DnaA boxes with respect

Table I. DNA sequences of DnaA boxes analysed in this study

pDOC170 fragments	Gene	DnaA box	Affinity[a]	5′ flanking	DnaA box 9 bp core	3′ flanking	K_D (nM)[b]
2130 bp		1[c]	High	ATACGG	TTATCCACA	GAATCA	nd
1363 bp	*dnaA*	1	Medium	AAGAGT	TTTTCCACA	CCTTCA	nd
1007 bp	*mioC*	R5	Medium	CCATAC	TTTTCCACA	GGTAGA	51
		R6[d]	Low	ATGTAC	TTATCAACA	AGATCC	nd
674 bp	*oriC*	R1	High	TCCTTG	TTATCCACA	GGGCAG	0.9
		M[e]	Low	CACCGA	TCATTCACA	GTTAAT	⩾2
		R2	Medium	GAGGGG	TTATACACA	ACTCAA	39
		R3	Low	CGGTAG	TTATCCAAA	GAACAA	⩾200
		R4	High	ACAGAG	TTATCCACA	GTAGAT	1.2
477 bp	*PdnaA*	1	High	CCCGAT	TTATCCACA	GGACTT	nd

[a]Affinities are classified high, medium and low, respectively, according to their determined K_D values (where possible) or as expected from their matching with the stringent definition of the DnaA box.
[b]K_D values were taken from Schaper and Messer (1995). nd, not determined.
[c]This DnaA box of pDOC170 corresponds to positions 2439–2437 of the pBR322 DNA sequence (GenBank accession no. J01749).
[d]Numbering of this DnaA box in *mioC* according to Christensen (1994).
[e]To avoid an ambiguous DnaA box nomenclature, we use 'M' for the *oriC* DnaA box found by Matsui *et al.* (1985). The arrangement of the DnaA boxes in *oriC* and *mioC* is shown schematically in the bottom part of Figure 5.

to the helix axis is important in the right part of *oriC*. In contrast, even 10 bp insertions between the AT-rich region and R1, or between R1 and M, or M and R2 result in non-functional origins (Messer *et al.*, 1992; Hsu *et al.*, 1994). In the left part of *oriC* not only the helical phasing of DnaA boxes is important but also their precise distance and the orientation of bound DnaA with respect to the DNA helix. Recently, ordered binding of DnaA to *oriC*, starting at DnaA box R4, has been observed using phenanthroline–copper footprinting (Margulies and Kaguni, 1996).

We were interested in how DnaA binding to the individual DnaA boxes is modulated by the *oriC* DNA sequence context. We studied DnaA binding to linear and supercoiled wild-type and mutant *oriC* DNA substrates *in vitro* by band-shift assays and electron microscopy. We show non-cooperative but ordered binding of DnaA to *oriC* with a special preference for R4, and define the DNA sequences required for this preference.

Results

DnaA binds sequentially to the DnaA boxes in oriC

We analysed the binding of DnaA protein at low and high protein concentrations (Figure 1, parts A and B) to purified *oriC* DNA fragments by a series of band-shift assays. Nucleoprotein complex formation between one DnaA molecule and one *oriC* DnaA box (complex I) already occurred at a DnaA concentration of 0.4 nM and a DnaA/DnaA box ratio of 0.02:1 (Figure 1A, lane 2). The definition of complex I as a DNA molecule having a single DnaA molecule bound to one DnaA box is based on the observation of monomeric binding of DnaA to DnaA boxes (Schaper and Messer, 1995). Free DNA was reduced to ~50% at a DnaA concentration of ⩽2 nM (Figure 1A, lane 6), close to the K_D value determined for *oriC* (Schaper and Messer, 1995). Small increments in DnaA concentration led to successive formation of complexes containing any number between one (Figure 1A, lanes 2–7) and six or more (lanes 6–13) DnaA molecules per DNA fragment. Apparently, binding of DnaA protein to linear *oriC* DNA is not cooperative, but proceeds sequentially.

At a DnaA/DnaA box ratio of 1:1 (Figure 1A, lane 11), no unbound DNA fragments were left and only traces of nucleoprotein complexes containing less than five DnaA molecules were detected. The formation of nucleoprotein complexes containing five DnaA molecules can be explained by monomeric binding of DnaA to R1, M, R2, R3 and R4. At protein concentrations exceeding a DnaA/DnaA box ratio of 10:1, nucleoprotein complexes could not be satisfactory resolved in this gel system (Figure 1B). The discrimination between specific DnaA oligomerization by protein–protein contacts at preformed smaller complexes and unspecific protein aggregation preventing proper electrophoretic migration of the samples was therefore impossible. In addition, protein–protein interaction is probably less stable during electrophoresis than protein–DNA interaction, resulting in the smeary band-shift pattern observed at higher protein concentrations (Figure 1A, lanes 11–13; Figure 1B, lanes 7–12). Saturation of DnaA binding to *oriC* was observed at DnaA/DnaA box ratios higher than 50:1 but precipitates of DnaA in the wells of the gels were not observed (Figure 1B). Extensive equilibration of DnaA with ADP or ATP concentrations in the reaction mixes of up to 2 mM did not alter the band-shift patterns obtained (not shown). The differences in complex formation at the same DnaA/DnaA box ratios seen in Figure 1A (100 μM ATP) and Figure 1B (2 mM ATP) were due to different final DnaA concentrations in the reactions and different incubation temperatures (see legend to Figure 1).

One DnaA box in oriC binds DnaA with unexpected high affinity

We probed the binding of *E.coli* DnaA protein to a set of DnaA boxes in a competition band-shift assay. DNA fragments containing one, two or five DnaA boxes, respectively, with different 9 bp core sequences in different sequence contexts were obtained in stoichiometric amounts by restriction of pDOC170 (see Table I). Nucleoprotein complex formation between DnaA and the *oriC* fragment

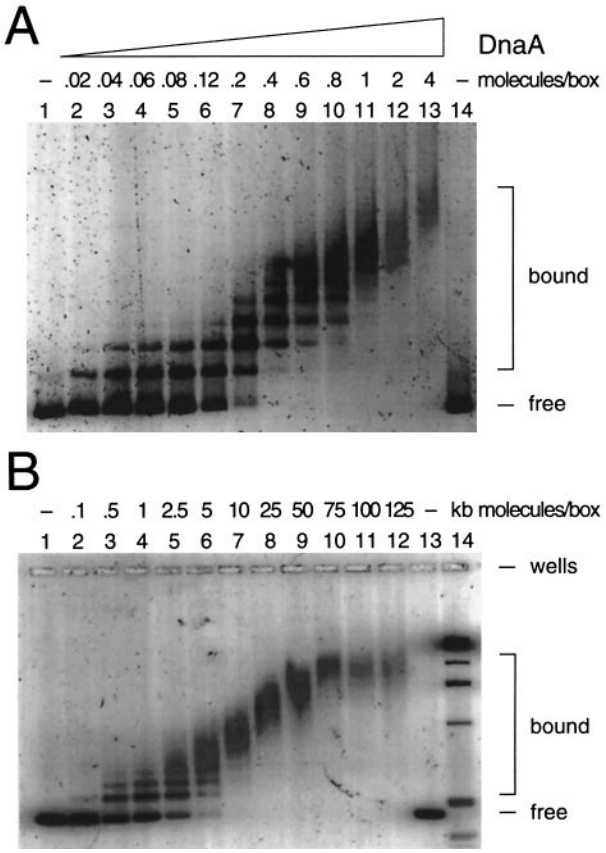

Fig. 1. DnaA binding to *oriC*. (**A**) 10 ng of a purified 461 bp *Sma*I–*Xho*I restriction fragment from pOC170 containing *oriC* (five DnaA boxes) were incubated with 100 µM ATP and increasing amounts of DnaA in reaction volumes of 10 µl for 10 min at 37°C. Lanes 1 and 14: without protein; lanes 2 to 13: 215 pg, 360 pg, 540 pg, 720 pg, 1.1 ng, 1.8 ng, 3.6 ng, 4.8 ng, 7.2 ng, 9 ng, 18 ng, and 36 ng, respectively. The ratio of DnaA molecules per DnaA box is indicated for each lane. Electrophoretic separation of the samples was allowed to proceed on a 2% agarose gel until the free DNA had reached a distance of 11 cm from the start point. (**B**) 4 ng of the same restriction fragment as in (A) were incubated in the presence of 2 mM ATP with increasing amounts of DnaA in reaction volumes of 10 µl for 10 min at 30°C. Lane 14: kb-ladder marker (Gibco-BRL, Bethesda, MA, USA); lanes 1 and 13: without protein; lanes 2 to 12: 360 pg, 1.8 ng, 3.6 ng, 9 ng, 18 ng, 36 ng, 90 ng, 187 ng, 275 ng, 363 ng, and 462 ng, respectively. The ratio of DnaA molecules per DnaA box is indicated for each lane. Electrophoretic separation of the samples was allowed to proceed on a 2% agarose gel until the free DNA had reached a distance of 6 cm from the start point.

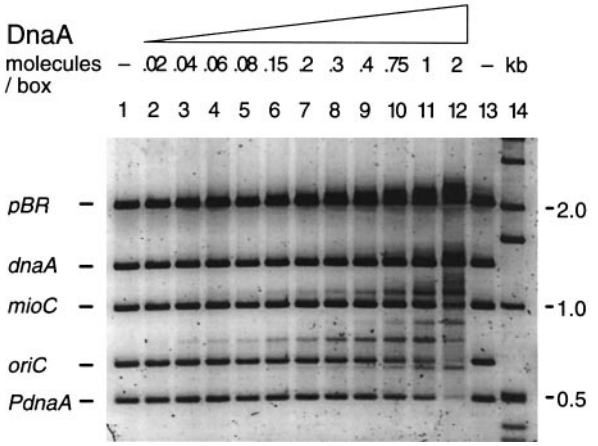

Fig. 2. Competition band-shift assay for plasmid pDOC170 (10 DnaA boxes). pDOC170 was double-digested with *Eco*RI and *Pst*I yielding fragments of 2130 bp (pBR322), 1363 bp (*dnaA*), 1007 bp (*mioC*), 674 bp (*oriC*) and 477 bp (*PdnaA*) in size (see Table I). 15 ng of the digest were incubated with increasing amounts of DnaA in 10 µl reactions for 15 min at 37°C. Lane 14: kb-ladder marker (Gibco-BRL); lanes 1 and 13: without protein; lanes 2 to 12: 30 pg, 80 pg, 120 pg, 160 pg, 300 pg, 400 pg, 600 pg, 800 pg, 1.5 ng, 2 ng, and 4 ng DnaA, respectively. The ratio of DnaA molecules per DnaA box is indicated for each lane. Electrophoretic separation of the samples was allowed to proceed on a 1% agarose gel until the 400 bp marker band had reached a distance of 14 cm from the start point.

was already visible at a DnaA/DnaA box ratio as low as 0.04:1 with a DnaA concentration of 150 pM in the assay (Figure 2, lane 3). At a DnaA/DnaA box ratio of ⩾0.1, complex formation was found to occur also for the *mioC*, *PdnaA* and pBR fragments (Figure 2, lanes 6 and 7). The *mioC* fragment contains one medium-affinity DnaA box (R5) and one box (R6) which does not match with the stringent consensus sequence (see Table I). However, it bound DnaA equally well as the *PdnaA* or pBR fragments, each containing one high-affinity DnaA box. DnaA binding to the low-affinity DnaA box located in the *dnaA* coding region was poor and only visible at the highest DnaA concentrations tested. In contrast to the experiment described above, binding of a second DnaA molecule to the *oriC* fragment (complex II) was only found at DnaA/DnaA box ratios higher than 0.3:1. This was surprising because *oriC* contains two high-affinity DnaA boxes (R1 and R4) and the medium-affinity box R2, and was thus expected to successfully out-compete the other fragments. Also, the mere accumulation of five DnaA boxes did not favour DnaA binding to the *oriC* fragment. We take this as indication that the *oriC* sequence context modulates the affinity for DnaA of the individual DnaA boxes more than was detectable by measuring their binding constants individually with oligonucleotides (Schaper and Messer, 1995). While one DnaA box in *oriC* bound DnaA considerably better than other competing high-affinity boxes, none of the remaining four DnaA boxes in *oriC* bound DnaA with a similar high affinity.

DnaA binds preferentially to box R4 in oriC

In order to identify the DnaA box with the highest affinity for DnaA in *oriC*, we carried out a different type of competition band-shift assay: a purified restriction fragment of pOC170–*oriC*$^+$ (fully *dam*-methylated) containing *oriC* and R5 in *mioC* was digested with *Hin*dIII to yield sub-fragments with R1, M, R2, R3 and R4 + R5, respectively (Figure 3). These sub-fragments were mixed in stoichiometric amounts with the unrestricted control fragment and assayed for DnaA binding. Formation of complex I was more efficient and observed at a lower DnaA/DnaA box ratio for the R4 + R5 fragment than for the fragment containing the remaining DnaA boxes in *oriC* (Figure 3, lanes 1–3). Since R5 is not a high-affinity box (Figure 2), we could identify R4 as the box with the highest affinity for DnaA. Formation of complex I was slightly more efficient at the control fragment than at the R4 + R5 fragment. This emphasizes that the *oriC* sequence between R3 + R4 contributes to the very high-affinity binding of R4, but that the 11 bp between the *Hin*dIII site (position 245; Buhk and Messer, 1983) and R4 are crucial.

The same sub-fragments as above were prepared from

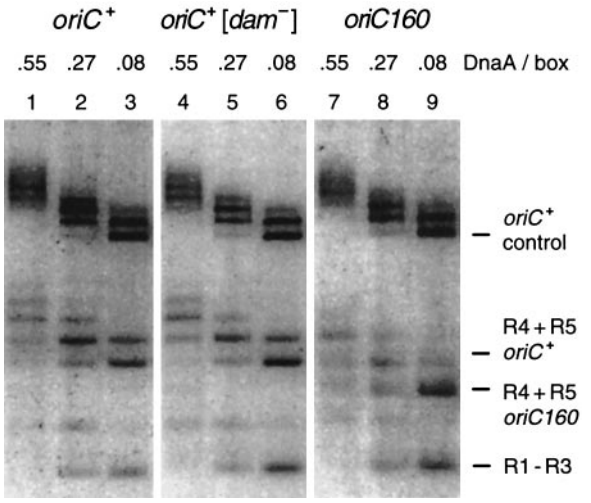

Fig. 3. Competition band-shift assay for *oriC* fragments. 5 ng of a 1074 bp *Mun*I/*Eco*RI fragment from plasmid pOC170–*oriC*$^+$ (six DnaA boxes) were mixed with 5 ng of a *Hin*dIII digest of this fragment (lanes 1–3), with 5 ng of a *Hin*dIII digest of the corresponding 1074 bp *Mun*I/*Eco*RI fragment from pOC170–*oriC*$^+$, isolated from *dam* strain WM1905 (lanes 4–6), or with 5 ng of a *Hin*dIII digest of the corresponding 997 bp *Mun*I/*Eco*RI fragment from pOC170–*oriC160* (lanes 7–9). The sizes of the sub-fragments were 426 bp (R1, M, R2, R3) and 648 bp (R4 + R5), respectively, except for the R4 + R5 fragment from *oriC160* which was 571 bp in size. The DNA mixtures were incubated with DnaA in 10 µl reactions for 15 min at 37°C; lanes 1, 4, 7: 1.24 ng; lanes 2, 5, 8: 0.62 ng; lanes 3, 6, 9: 0.38 ng. The ratio of DnaA molecules per DnaA box is indicated for each lane. Electrophoretic separation of the samples was allowed to proceed on an 1% agarose gel until the 400 bp marker band had reached a distance of 14 cm from the start point. A wider range of DnaA/DnaA box ratios was tested experimentally but found to appear virtually identical with respect to complex formation. Hence, this figure shows only representative parts of the gels.

unmethylated pOC170–*oriC*$^+$ and from pOC170–*oriC160* (deletion to the right of R4); these sub-fragments were assayed in competition with the fully *dam*-methylated unrestricted *oriC*$^+$ fragment (Figure 3, lanes 4–6 and 7–9, respectively). The band-shift patterns were virtually identical in all three assays. We take this as indication that neither *dam* methylation nor the curved DNA segment to the right of *oriC* have any detectable influence on DnaA binding to R4.

Analysis of DnaA–oriC nucleoprotein complexes by electron microscopy

A straightforward experimental approach to define the sequential order of DnaA binding to DnaA boxes in *oriC* is the analysis of DnaA–*oriC* nucleoprotein complexes by electron microscopy. In order to evaluate our protocol, we analysed the binding of DnaA to a 1087 bp DNA fragment containing the DnaA box from the *dnaA* promoter region. At a DnaA/box ratio of 6:1, we found nucleoprotein complexes of varying sizes but almost exclusively at positions corresponding to the DnaA box within a range of ±40 bp from its central base pair (Figure 5, panel A). This result shows that, under our conditions, DnaA binding to a single-box fragment is sufficiently specific. However, the size variation of the complexes is indicative of DnaA–DnaA interactions, and responsible for the broadening of the peak because larger complexes could be measured less accurately. Therefore, lower DnaA concentrations were used for the analysis of DnaA binding to the closely spaced DnaA boxes in *oriC*.

We analysed DnaA binding to a 1308 bp DNA *oriC*$^+$ fragment carrying in addition to *oriC* both *mioC* DnaA boxes, R5 + R6 (Christensen, 1994). At a DnaA/box ratio of 1.5:1, nucleoprotein complexes were found at positions corresponding to all seven DnaA boxes on the fragment, albeit with different frequencies; complexes at the position of R4 were most frequent (Figure 5, panel B). The majority of DNA fragments had one complex bound; fragments with two to three complexes at different positions were found with frequencies below 20%. The high frequency of complexes at R6 was not entirely reproducible (see Figure 5, panels F, H, L) but surprising because this DnaA box does not match the stringent definition (see Table I). However, efficient competition of fragments carrying high-affinity DnaA boxes by the *mioC* fragment was already observed in the band-shift analysis (Figure 2). It transpired during the course of this study that having DnaA boxes from the *mioC* promoter region (see Table I) on *oriC* fragments was advantageous since it provided us with an internal standard when analysing mutant *oriC* substrates (see below). We found small nucleoprotein complexes of varying sizes already at a DnaA/DnaA box ratio of 0.5:1, although at this DnaA concentration the majority of DNA molecules was devoid of any bound protein. It was therefore impossible to determine the dimensions of the 'monomer complex' with certainty.

An order of DnaA binding to linear oriC DNA?

We extended the analysis of DnaA–*oriC* nucleoprotein complexes by electron microscopy in three directions: (i) DnaA binding to linear *oriC* fragments at increasing protein concentrations; (ii) DnaA binding to *oriC* mutants; and (iii) DnaA binding to supercoiled *oriC*.

A possible binding order of DnaA to the DnaA boxes in *oriC* was analysed by determining the positions of nucleoprotein complexes formed at increasing DnaA concentrations on a 1074 bp restriction fragment from pOC170 carrying *oriC* and R5 in *mioC*. Electron micrographs of representative molecules are shown in Figure 4 (panels a–c). At DnaA/DnaA box ratios of 1:1 and 2:1, nucleoprotein complexes at the position of R4 were most frequent, in support of the results from the band-shift analysis that DnaA binds preferentially to R4 (Figure 4, panels A–C; see also Figure 5, panel B). Nucleoprotein complexes at the position of R1 were found less frequently than complexes at low-affinity box R5. This is in line with the observation from the band-shift analysis that R1 in the *oriC* context binds DnaA protein with lower affinity than expected from its binding constant. At a DnaA/DnaA box ratio of 1:1, a shoulder on the left side of the prominent 'R4 peak' indicated DnaA binding to R2 and R3 to apparently the same extent as to R1 (Figure 4, panels B and E). Nucleoprotein complexes were also found in the region of DnaA box M. However, due to their low frequency, their unambiguous assignment to M was only possible at the higher DnaA/DnaA box ratios.

Assuming that the frequency of nucleoprotein complexes found at the five *oriC* boxes reflects an order of binding, we conclude that DnaA binds first to R4. Consecutively, DnaA binds with no measurable preference to either R1, R2 or R3. DnaA binding to box M occurs

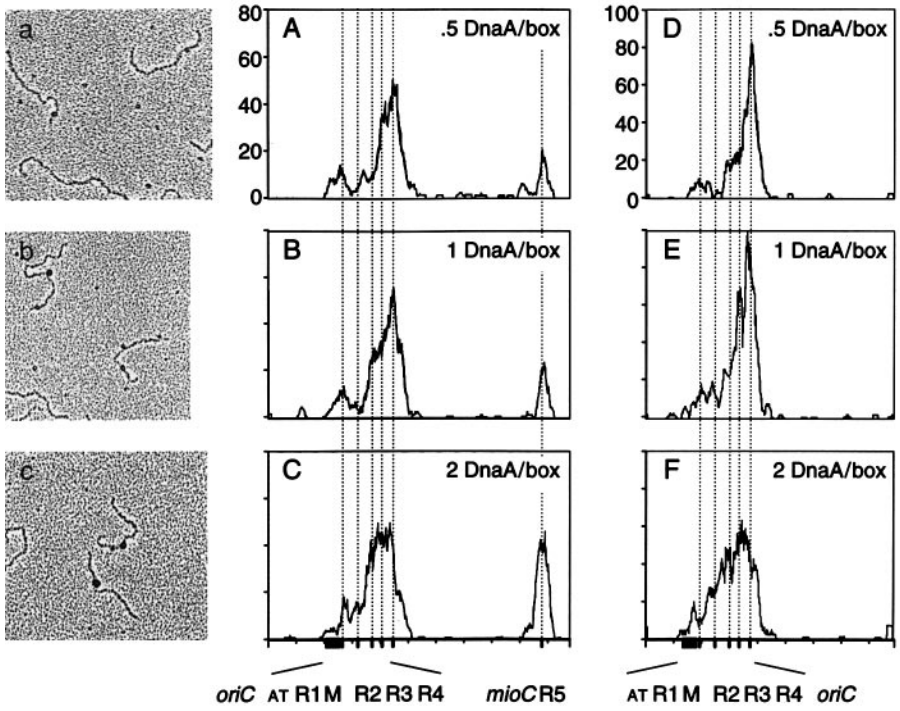

Fig. 4. The order of DnaA binding to linear *oriC* DNA. Electron micrographs of representative molecules a–c and histograms A–C show binding of DnaA to a 1074 bp *Eco*RI/*Mun*I *oriC* fragment from pOC170 (six boxes). (**a**, **A**) amount of DnaA used corresponds to 0.5 DnaA/box, individual DNA molecules represented in the histogram, $n = 258$; (**b**, **B**) 1.0 DnaA/box, $n = 278$; (**c**, **C**) 2.0 DnaA/box, $n = 271$. Histograms D–F show binding of DnaA to a 890 bp *Aat*II/*Afl*III *oriC* fragment from pOC170 (five boxes). (**D**) 0.5 DnaA/box, $n = 251$; (**E**) 1.0 DnaA/box, $n = 379$; (**F**) 2.0 DnaA/box, $n = 297$. The relative positions of the AT-rich region in *oriC* (indicated by 'AT'; shaded box) and the DnaA boxes (indicated by R1–R5, thick line) with respect to the ends of the fragments is indicated in the lower part of the figure for the two *oriC* fragments. The DNA fragments were blunt-ended by treatment with T4 DNA polymerase before electron microscopic analysis. For details of binding reactions and electron microscopic analysis, see Materials and methods.

last. Complex formation in the R2/R3/R4 region, resulting in a broad peak, seems to be favoured over DnaA binding to R1 and M at a DnaA/DnaA box ratio of 2:1. However, this is probably a consequence of increasing possibilities for DnaA–DnaA contacts at preformed DnaA–DnaA box complexes at these closely spaced boxes rather than of a higher affinity for DnaA of R2 and R3 as compared with box R1. An unambiguous binding order for R1, R2 and R3 could therefore not be determined. At DnaA concentrations exceeding a DnaA/DnaA box ratio of 2:1, the nucleoprotein complexes formed became too bulky to pinpoint reliably their binding to particular DnaA boxes. The notion of possible DnaA–DnaA interactions was substantiated by the frequent observation of loop formation due to interaction between nucleoprotein complexes at the *oriC* and *mioC* regions of individual DNA molecules at higher DnaA/DnaA box ratios (not shown).

The experiment was repeated with a different DnaA preparation and a 890 bp restriction fragment lacking R5 from pOC170. The results described above could be reproduced (Figure 4, panels D–F). In one case, the data shown in the histogram (Figure 4, panel E) were analysed in more detail: 379 DNA molecules with nucleoprotein complexes were measured for their apparent length, which varied by not more than 5.1%. The length variation of this DNA fragment treated in the same way but not complexed with DnaA protein was 3.9%. Among the 379 molecules, 334 (~90%) showed one nucleoprotein complex, while 43 molecules (11.3%) showed complexes at two distinct positions; two molecules showed complexes at three positions. In this particular experiment, a reliable determination of the binding order seemed possible because artefactual results due to DnaA–DnaA oligomerization at the closely spaced DnaA boxes (see above) would be reduced to a minimum. Of the 334 molecules with one complex, 215 (64.5%) showed a complex at a position corresponding to R4, 19 (5.7%) at R1, 18 (5.5%) at M, 30 (9%) at R2, 25 (7.3%) at R3, and 27 (8%) at unspecific positions. Of the 43 molecules with two complexes, 17 (40%) showed one complex at a position corresponding to R4 and a second complex at the position of R1 (six), R2 (two), R3 (six) or at unspecific positions (three). Although preferential DnaA binding to R4 is once again emphasized by this analysis, we consider DnaA binding to boxes R1, R2 and R3 as random.

DnaA binding to oriC mutants

The analyses described so far failed to detect any cooperativity of the DnaA–*oriC* interaction. This issue was therefore addressed by electron microscopic analysis of DnaA binding to several well-characterized *oriC* mutants (Langer *et al.*, 1996), and in a complementary approach, by analysis of binding of a β-galactosidase::DnaA fusion protein and DnaA508 mutant protein to wild-type *oriC*.

Nucleoprotein complex formation at positions corresponding to R4 was completely abolished on *oriC10* (mutation of R4) and *oriC163* (deletion of R4) substrates (Figure 5, panels C and E). However, nucleoprotein complex formation was not altered at the remaining boxes. This adds support to our notion of non-cooperative DnaA

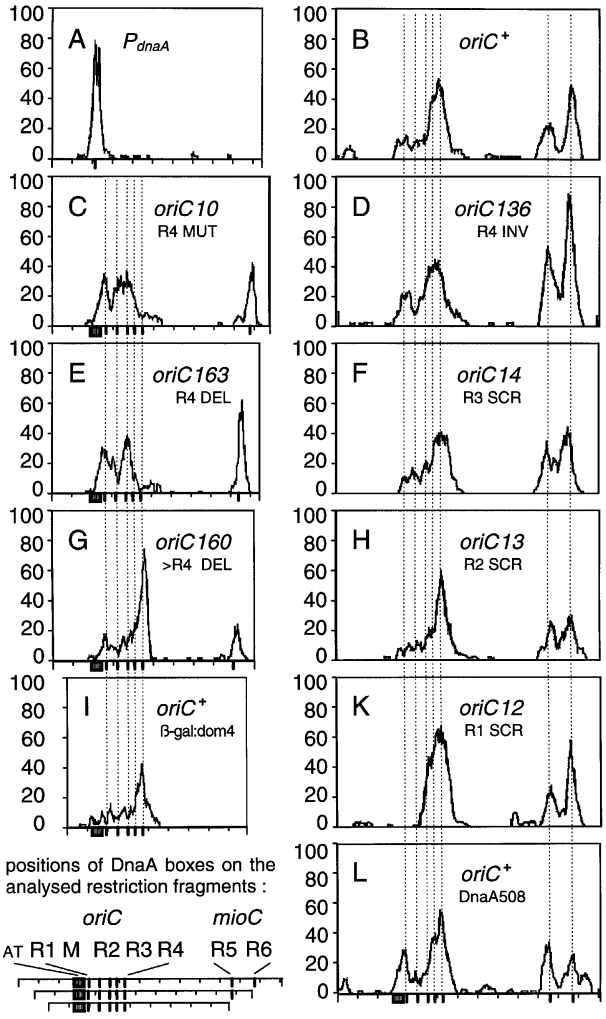

Fig. 5. DnaA binding to *PdnaA*, wild-type *oriC* and *oriC* mutants. Histograms: (**A**) Binding of DnaA to *PdnaA*, amount of DnaA used corresponds to 6 DnaA/box, individual DNA molecules represented in the histogram, $n = 257$; (**B**) binding of DnaA to wild-type *oriC*, 1.5 DnaA/box, $n = 229$; (**C**) *oriC10* (R4 point mutation), 0.5 DnaA/box, $n = 240$; (**D**) *oriC136* (R4 inverted) 1.5 DnaA/box, $n = 416$; (**E**) *oriC163* (R4 deleted), 0.5 DnaA/box, $n = 252$; (**F**) *oriC14* (R3 scrambled), 0.5 DnaA/box, $n = 278$; (**G**) *oriC160* (deletion to the right of *oriC*), 0.5 DnaA/box, $n = 236$; (**H**) *oriC13* (R2 scrambled), 0.5 DnaA/box, $n = 239$; (**I**) binding of a β-gal:dom4 fusion protein to wild-type *oriC*, DnaA/box ratio uncertain due to only partially purified protein, $n = 173$; (**K**) *oriC12* (R1 scrambled), 1.5 DnaA/box, $n = 300$; (**L**) binding of DnaA508 protein to wild-type *oriC*, 1.5 DnaA/box, $n = 276$. For simplicity, the DnaA/box ratios used experimentally and indicated here were calculated assuming wild-type binding properties also for the mutant fragments. Restriction fragments used in this experiment were: (i) 1087 bp *Pme*I/*Eco*RV from pDOC170 containing the *PdnaA* DnaA box (A); (ii) 890 bp *Aat*II/*Afl*III (*oriC*, five boxes) from pOC170 (I); (iii) *Eco*RI/*Mun*I (*oriC* + *mioC*, six boxes) from pOC170–*oriC10* (1074 bp), pOC170–*oriC163* (1036 bp) and pOC170–*oriC160* (997 bp) (C, E and G, respectively); (iv) 1308 bp *Hae*II (*oriC* + *mioC*, seven boxes) from pOC170 (B+L), pOC170–*oriC136* (D), pOC170–*oriC14* (F), pOC170–*oriC13* (H), pOC170–*oriC12* (K). The relative positions of the AT-rich region in *oriC* (indicated by 'AT'; shaded box) and the DnaA boxes (indicated by R1–R5, thick line) with respect to the ends of the fragments is indicated. Where necessary, the DNA fragments were blunt-ended by treatment with T4 DNA polymerase before electron microscopic analysis. For details of binding reactions and electron microscopic analysis, see Materials and methods.

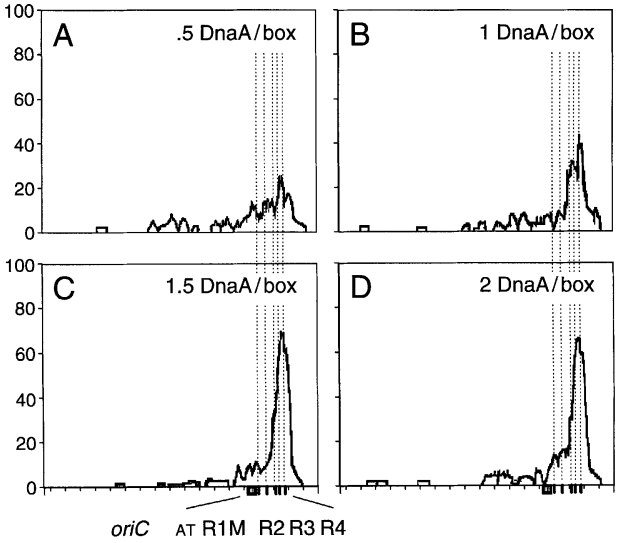

Fig. 6. DnaA binding to supercoiled *oriC* DNA. Supercoiled pOC170 DNA (>80% ccc form) was incubated with DnaA under binding conditions as described in Materials and methods. Following fixation, the DNA was linearized with *Ssp*I and *Pst*I, and blunt-ended by treatment with T4 DNA polymerase before electron microscopic analysis. Nucleoprotein complexes were almost exclusively found on the 1837 bp fragment containing *oriC*. Histograms: (**A**) amount of DnaA used corresponds to 0.5 DnaA/box, individual DNA molecules represented in the histogram, $n = 125$; (**B**) 1.0 DnaA/box, $n = 141$; (**C**) 1.5 DnaA/box, $n = 187$; (**D**) 2.0 DnaA/box, $n = 178$. The relative positions of the AT-rich region in *oriC* (indicated by 'AT'; shaded box) and the DnaA boxes (indicated by R1–R5, thick line) with respect to the ends of the fragments is indicated in the lower part of the figure.

binding to *oriC*. A similar affinity for DnaA binding was expected and found for R2 and R5, but once again R1 showed a lower affinity in the *oriC* context than expected (see Table I). These results show, in addition, that the shoulder always observed within the prominent 'R4 peak' on wild-type *oriC* substrates at positions corresponding to R2 and R3 truly represents DnaA bound to these positions (Figure 5, panel B; see also Figure 6).

DnaA did not bind preferentially to R4 on an *oriC136* substrate, in which R4 is inverted relative to the flanking bases. In this case we found a similar affinity of DnaA for R2, R3, R4 and R5 (Figure 5, panel D). We take this as indication that the specific sequence context resulting in preferential DnaA binding to box R4 is operative only in the 'correct' orientation of the 9-mer sequence, while the inversion of the 9-mer had no detectable influence on DnaA binding to the remaining DnaA boxes in *oriC*. We found by band-shift analysis that sequences to the right of *oriC* are not required for preferential DnaA binding to R4. This result was confirmed by electron microscopic analysis of *oriC160* (deletion of positions 275–352) (Figure 5, panel G). Interestingly, the broadened basis to the right side of the prominent 'R4 peak' was not found for *oriC160*, pointing to unspecific DnaA binding to the curved DNA segment to the right of wild-type *oriC* (Figure 5, compare panels B, C and G; see also Figure 4).

Nucleoprotein complexes at positions corresponding to R2 and R3 could not be resolved clearly on wild-type *oriC* substrates and were therefore analysed on appropriate mutant substrates. The nucleoprotein complex distribution on *oriC13* (inactivated R2) closely resembled that of wild-

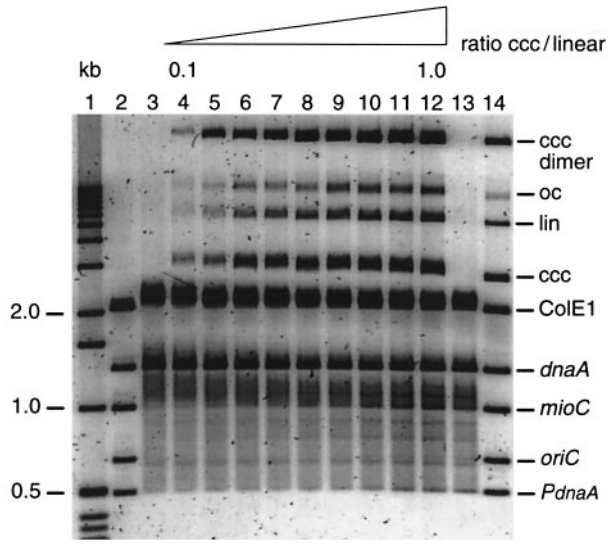

Fig. 7. Competition band-shift assay of linearized and supercoiled pDOC170. Plasmid pDOC170 (10 DnaA boxes) was double-digested with *Eco*RI and *Pst*I as described in the legend to Figure 1. 30 ng of the double digest were incubated with increasing amounts of ccc form of pDOC170 (~80% ccc monomer + dimer, ~20% linear and oc form) with 5.7 ng (lanes 3–12) or 2.85 ng (lane 13) of DnaA in 10 µl reactions for 15 min at 37°C. Lane 1: kb-ladder marker (Gibco-BRL); lane 2: digest without protein; lanes 3 and 13: digest with protein; lanes 4–12: addition of 2 ng, 4.25 ng, 6.5 ng, 8.72 ng, 11 ng, 13.25 ng, 15.5 ng, 17.75 ng, and 32 ng ccc form, respectively; lane 14: digest and 11 ng ccc-form without protein. The ratio of DnaA molecules per DnaA box with respect to the digest was 1.25:1 for lanes 3–12, and 0.65:1 for lane 13. For the *PdnaA*, *oriC*, *mioC*, *dnaA* and *Col*E1 fragments, only the position of the faster-running free DNA is indicated. Electrophoretic separation of the samples was allowed to proceed on an 1% agarose gel until the 400 bp marker band had reached a distance of 14 cm from the start point.

type *oriC* at the same DnaA/box ratio (Figure 5, panel H; compare with panel B). Therefore, DnaA binding to the low-affinity box R3 also contributes to the pronounced shoulder of the 'R4 peak' (Figure 5, panel B). A distinct peak at the position corresponding to R2 was found on *oriC14* (inactivated R3) pointing to roughly equal affinity of DnaA for R1 and R2 (Figure 5, panel F). On *oriC14*, preferential DnaA binding to R4 was not observed. Apparently, the wild-type sequence of the R3 region is necessary to allow preferential DnaA binding to box R4 in the *oriC* context. This is, however, the only case where we found that a mutation in one *oriC* DnaA box altered the affinity for DnaA of another box.

Nucleoprotein complex formation was observed several times—though not reproducibly—at positions corresponding to the AT-rich 13-mers to the left of R1 (Figure 5, panel B). Nucleoprotein complexes at this position were clearly absent on *oriC12* with inactivated R1 (Figure 5, panel K). As observed for the other *oriC* mutant substrates, DnaA binding to the remaining DnaA boxes was not affected by the mutation of R1.

We were interested in whether DnaA protein itself contributes to the observed DnaA box preference. The 94 C-terminal amino acid residues of DnaA fused to β-galactosidase were shown to be sufficient yet necessary for specific DNA binding (Roth and Messer, 1995). This fusion protein bound with the same preference to the DnaA boxes in *oriC* as wild-type DnaA (Figure 5, panel I). The mutant protein DnaA508 (P27L, T79I in domain 1) was found to be completely inactive in the *in vitro* replication assay unless supplemented with small amounts of wild-type DnaA (A.Schmidt, unpublished results). However, DnaA508 protein bound to DnaA boxes in *oriC* indistinguishable from wild-type DnaA (Figure 5, panel L). These results strongly suggest that domains 1–3 of DnaA protein are not involved in determining DnaA box preference.

DnaA binds with the same affinity to linear and supercoiled oriC DNA

In addition to the sequence context, the topology of *oriC* might be important for determining the DnaA box preference. DnaA was bound to pOC170 (ccc-form) and the resulting nucleoprotein complexes fixed by glutaraldehyde treatment. Subsequently the plasmid DNA was linearized by digestion, the samples mounted on grids, and analysed by electron microscopy (Figure 6). Binding of DnaA to pOC170 was achieved in these experiments by a 1-min treatment at 37°C in order to minimize plasmid relaxation by traces of topoisomerase I contaminations in our DnaA preparation. At low DnaA concentrations, specific nucleoprotein complex formation in the *oriC* region was only marginally more frequent than unspecific binding (Figure 6, panel A). With slightly increasing DnaA concentrations, the distribution of nucleoprotein complexes became virtually identical to those obtained with linear fragments as substrate (Figure 6, panel D). Also on the supercoiled substrate, DnaA binding occurred preferentially at R4 (Figure 6, panel B). Nucleoprotein complex formation in the R2/R3/R4 region was clearly more prominent than complex formation at R1 or M. The significant degree of unspecific binding may account for the observation that slightly higher DnaA concentrations were necessary in these experiments to obtain nucleoprotein complex distributions comparable with those obtained with linear fragments. In a control experiment, DnaA protein purified from a *topA* strain gave identical results (not shown).

Although the order of DnaA binding to individual DnaA boxes in *oriC* was not influenced by the topology of the DNA substrate, the efficiency of binding to DNA might still have differed. Since analysis by electron microscopy was not suitable to detect such differences, we carried out a different type of competition band-shift assay: titration of nucleoprotein complexes formed on restriction fragments of pDOC170 by increasing amounts of added ccc-form of this plasmid (Figure 7). As controls, linear fragments only were incubated with the same amount of DnaA, or with half the amount of DnaA (Figure 7, lanes 3 and 13). In the competition, the reappearance of free fragments was indicative of successful competition of the linear fragments and ccc-form DNA for DnaA (Figure 7, lanes 4–12). At a molar ratio of linear fragments to ccc-form of 1:1 (Figure 7, lane 12), the band-shift pattern obtained in the competition was virtually indistinguishable from that of the control in lane 13. We conclude from the results of both experimental approaches that DnaA binds with the same box preference and equally well to linear and ccc-form DNA, i.e. DnaA binding to *oriC* is determined by the DNA sequence context rather than by the topology.

Discussion

We have analysed by band-shift assays and electron microscopy the binding of *E.coli* DnaA to the replication origin, *oriC*. We have obtained clear evidence that DnaA binds with the same affinity to linear or supercoiled DNA (Figure 7). We could show, in addition, that the binding order of DnaA to individual DnaA boxes in *oriC* is virtually identical on linear or supercoiled substrates. Our results corroborate those from earlier 'footprint' analyses of the DnaA–DNA interaction that failed to reveal striking differences for the protection patterns obtained *in vivo* on the natural substrate or *in vitro* on fragments (Samitt *et al.*, 1989). The *in vitro* replication systems for *E.coli* depend on a high degree of negative superhelicity of a plasmid-borne *oriC* substrate (Fuller *et al.*, 1981). From our results we conclude that this dependency is mainly due to the need for unwinding of the AT-rich region for replication to occur. It seems clear, however, that the first step of initial complex formation, the binding of DnaA to individual DnaA boxes in *oriC*, may well be studied *in vitro* on linear substrates.

Both approaches employed in this study failed to reveal any cooperativity of the DnaA–*oriC* interaction. A steady increase in complex sizes by cumulative binding of DnaA monomers to the *oriC* substrate was reproducibly observed with increasing protein concentrations (Figure 1 and Figure 4, panels A–C). The analysis of mutant *oriC* substrates revealed that mutations of individual boxes changed or prevented the binding of DnaA to the respective box but did not, with the exception of *oriC14* (see below), alter the binding preferences to the remaining boxes. The observation of identical box preference of wild-type DnaA and the β-galactosidase::DnaA (domain 4) fusion protein supports our notion that the DnaA–*oriC* interaction is non-cooperative. Also, the K_D value determined for the DnaA–*oriC* interaction did not suggest cooperative binding when compared with the K_D values of the individual DnaA boxes (Schaper and Messer, 1995).

For all wild-type *oriC* fragments analysed in this study, R4 bound DnaA not only considerably better than R1 or the other boxes in *oriC*, it also out-competed other R1/R4-type boxes by a factor of three in a competition band-shift assay (Figure 2). Preferential binding of DnaA to R4 in *oriC* was also found by Margulies and Kaguni (1996) using phenanthroline–copper footprinting. By band-shift analysis of appropriate restriction fragments and mutant *oriC* substrates (Figure 3) we could show that preferential DnaA binding to R4 (positions 260–268) depends on positions 249 to 274 of the *oriC* DNA sequence (coordinates refer to Buhk and Messer, 1983). However, only the wild-type *oriC* sequence of the R3 region (~40 bp upstream of R4) and the 'correct' orientation of R4 allowed preferential binding to R4, as revealed by analysis of *oriC14* and *oriC136*, respectively. Interestingly, DNA restriction fragments of these mutants exhibit a lower degree of intrinsic curvature than wild-type fragments (H.Seitz and C.Weigel, unpublished results). On the other hand, preferential binding of DnaA to R4 was independent of *dam* methylation, and also independent of the intrinsically curved DNA segment to the right of *oriC* as revealed by analysis of *oriC160*. Taken together, these results point to a particular DNA structure necessary to achieve high-affinity binding of DnaA to R4. However, the clustering of DnaA boxes in the right part of *oriC* may enhance this effect by increasing the probability for successful DnaA–DNA contacts within a short stretch of DNA. Five DnaA boxes were found on the *E.coli* chromosome which also show an unusually high affinity for DnaA (A.Roth and W.Messer, unpublished results). These boxes are of the R1/R4 or R2 type, but none of them is part of a DnaA box cluster. Apparently, clustering of DnaA boxes is not required to increase the affinity for DnaA of a particular box above the normal level. The particular biological importance of such very high-affinity DnaA boxes is presently unknown.

Although rather suggestive from the *in vitro* analysis, a 'pacemaker' function of R4 for initial complex formation *in vivo* should be discussed with all necessary caution: minichromosomes carrying *oriC14*, *oriC136* (loss of preferential DnaA binding to R4) or *oriC10* (no DnaA binding to R4 *in vitro*) replicate efficiently in host strains with wild-type chromosomal *oriC* (Langer *et al.*, 1996). Moreover, an *E.coli* mutant having R4 deleted from its chromosomal replication origin is viable and replicates from *oriC* (Bates *et al.*, 1995). However, minichromosomes carrying *oriC163* (deletion of R4) cannot successfully replicate in a wild-type host, demonstrating the severe consequences of this mutation (Langer *et al.*, 1996).

Two lines of evidence suggest that binding to R1, R2 or R3 is random: (i) the statistical analysis of the histogram presented in Figure 4, panel E, did not reveal a significant preference for either of the three boxes, besides the preference for R4; and (ii) the analysis of *oriC* substrates with deleted or inactivated R4 showed a similar distribution of DnaA bound to R1, R2 or R3 (see Figure 5, panels C and E). Only M was bound with the lowest affinity in the majority of experiments. We therefore propose for binding of DnaA to *oriC* the order: R4 > (R1, R2, R3) > M. The low affinity of R1 is at variance with results obtained using phenanthroline–copper footprinting of DnaA–*oriC* complexes separated by gel electrophoresis (Margulies and Kaguni, 1996). DnaA–*oriC* complexes analysed by electron microscopy in this study were fixed immediately following complex formation, which avoids possible rearrangements during electrophoresis. Also, the DnaA protein used here was purified without a denaturation step, resulting in a protein which was not prone to self-aggregation. Mutant *oriC* substrates were analysed in addition to wild-type *oriC*, thus giving a broader data basis for evaluation of the results.

Our results show unambiguously that R1 has a reduced affinity for DnaA in the *oriC* context. This was unexpected since the DnaA binding constants were identical for R1 and R4 when determined using 21-mer oligonucleotides with 6 bp cognate *oriC* sequence on either side of the DnaA boxes (see Table I) (Schaper and Messer, 1995). In the *oriC* context, R1 and R2 bound DnaA with approximately equal affinity. The extension of the flanking sequences responsible for this effect have yet to be determined. Possible structural alterations of *oriC* due to DnaA binding to R2, R3 or R4, or—at slightly higher DnaA concentrations—due to the formation of larger nucleoprotein complexes covering the R2–R4 region, do not increase the probability of DnaA binding to R1 (see Figure 4). Again,

this finding is in line with our notion of non-cooperative binding of DnaA to *oriC*.

It has been proposed that from initial to open complex is triggered by DnaA binding to a low-affinity box in *oriC* (Samitt *et al.*, 1989). Of all *oriC* DnaA boxes, M showed the lowest affinity in our analyses. This makes M a novel candidate for a 'regulatory' box, a quality so far proposed for R3. In contrast to R3, mutations of the box-inversion or box-inactivation type in M result in non-functional origins, emphasizing its importance for *oriC* function (Langer *et al.*, 1996). On the other hand, R3 was shown to be covered with DnaA at a specific time point in the cell cycle, coincident with replication initiation (Cassler *et al.*, 1995).

With respect to box preference in binding to *oriC* we found no differences between wild-type DnaA, DnaA508 protein and a β-galactosidase::DnaA (domain 4) fusion protein. Also DnaA protein of *Bacillus subtilis* bound to the *E.coli oriC* with the same box preference as did *E.coli* DnaA (M.Krause and W.Messer, unpublished results). The DnaA508 mutant protein is therefore not defective in initial complex formation. The result obtained with the β-galactosidase::DnaA (domain 4) fusion protein demonstrates that domains 1–3 of DnaA are not involved in determining the observed box preference, emphasizing a modular architecture of DnaA protein.

We have analysed the binding of purified DnaA to *oriC in vitro*. Within the living cell, *oriC* also interacts specifically with a chamber orchestra of other proteins, namely HU, IHF, Fis, Rob, IciA, SeqA, H-NS and Dam methyltransferase (Messer and Weigel, 1996). All these interactions modulate in a cell cycle-dependent manner the structure of *oriC* and the binding of DnaA to *oriC* (Cassler *et al.*, 1995). Only a multi-factor analysis will therefore allow to describe in molecular terms the highly regulated formation of the initial complex and its transition to the open complex. The basic biochemical reaction, however—the DnaA-dependent DNA unwinding in the AT-rich 13-mer region in the left part of *oriC*—can be achieved without additional factors *in vitro*, albeit somewhat inefficiently (Hwang and Kornberg, 1992). Knowledge of the order of binding of DnaA to its five binding sites in *oriC* may therefore support future efforts: (i) to measure the stress to which the *oriC* DNA is subjected by these interactions at individual DnaA boxes; and (ii) to understand how this localized stress within the DNA helix is transmitted to the left part of *oriC* where the helical distortions become manifest as DNA unwinding.

Materials and methods

DnaA purification

DnaA protein was overproduced in *fis*(Null) strain WM2121 (*ara* Δ*lac-pro fis::Km recA56 rpsL srlC300::Tn10 thi*) or *topA* strain WM2311 (*gal-25 nirR pyrF287 rpsL195 thi topA10*) from expression vector pdnaA116 (M.Krause and W.Messer, submitted). DnaA was purified as described except that 100 mM potassium glutamate was used instead of KCl (Schaper and Messer, 1995). DnaA508 protein was overproduced in *dnaA*(Null) strain WM1940 (*argH deo dnaA850::Tn10 his-29 ilv metB metD88 pro rnh::Cm thyA trpA9605*) (Kline *et al.*, 1986) from a pdnaA116 derivative carrying the *dnaA508* allele (to be published elsewhere). A denaturation step was included in the purification scheme for this protein (Sekimizu *et al.*, 1988b). Purified β-galactosidase::DnaA (domain 4) fusion protein was kindly provided by A.Roth (Roth and Messer, 1995).

Strains and plasmids

Plasmid pOC170 (3852 bp) contains *oriC* sequences from –176 to +1497, the ColE1 *rop* replication origin of pBR322 on a *Not*I cassette, and the *bla* gene from pT7-7 for selection (Messer *et al.*, 1992). Plasmid pDOC170 contains in addition a functional *dnaA* gene including the entire promoter region (positions 578–2404, GenBank accession No. J01602) cloned between the *Sal*I and *Sac*I sites of pOC170. pOC170–*oriC160* was obtained by restriction of pOC170 with *Hin*dIII and *Bcl*I and replacement of the 107 bp fragment with a synthetic ds-oligodeoxyribonucleotide leaving a deletion of positions 275 to 352; *oriC* DNA fragments from pOC170–*oriC160* have almost entirely lost the intrinsic curvature found to be centred around position 315 (not shown) (Kimura *et al.*, 1989). pOC170–*oriC10* carries two point mutations in box R4, rendering this site refractory to DnaA binding (Holz *et al.*, 1992). Plasmids pOC170–*oriC12*, pOC170–*oriC13* and pOC170–*oriC14* carry inactivating mutations in DnaA boxes R1, R2 or R3, respectively; plasmid pOC170–*oriC136* carries an inversion of DnaA box R4 (Langer *et al.*, 1996). pOC170–*oriC163* was obtained by restriction of pOC170 with *Hin*dIII and *Bsp*1107 I, flushing of the ends and religation, thus eliminating box R4. Plasmid DNAs were prepared routinely from XL1-blue (*endA1 gyrA46 hsdR17 lac recA1 relA1 supE44 thi*; F′lac: $lacI^{Q}$ $lacZ\Delta M15$ *Tn10* $proAB^{+}$) or WM1905 (*dam-13::Tn9 dcm hsdR mcrA mcrB*) transformants using QIAGEN purification kits (QIAGEN, Hilden, Germany). DNA restriction fragments were purified from agarose gels with the QIAquick purification kit (QIAGEN) and found to be sufficiently pure for electron microscopic analysis. DNA-modifying enzymes were from Boehringer-Mannheim (Germany) and used as recommended by the manufacturer.

Band-shift assay

Binding of *E.coli* DnaA protein to DNA was analysed by band-shift assays on agarose gels (Seakem LE; FMC, Rockland ME, USA). Aliquots of DnaA were thawed, adjusted to a final concentration of 100 μM ATP, and diluted into binding buffer (20 mM HEPES–KOH, pH 8.0, 5 mM Mg-acetate, 1 mM EDTA, 4 mM DTT, 0.2% Triton X-100, 5 mg/ml bovine serum albumin, 5% glycerol, 100 μM ATP) (Parada and Marians, 1991). DnaA dilutions were active when kept on ice for up to 3 days. Assay mixtures (usually 10–20 μl) were assembled by adding an equal volume of the desired protein dilution to 10 pg to 100 ng DNA in H_2O on ice. Binding of DnaA to DNA was achieved by incubation of the reaction at 37°C for 10 min unless indicated otherwise. Electrophoresis was carried out at room temperature in 0.5×TBE buffer (22.5 mM Tris–borate, 0.5 mM EDTA, pH 8.0) at 4 V/cm. Gels were stained with SYBR-GREEN (Molecular Probes Europe, Leiden, Netherlands) in electrophoresis buffer according to the manufacturer's instructions. Stained gels were read with the FluorImager 575 and processed with ImageQuant NT/3.3 software (Molecular Dynamics, Krefeld, Germany).

Electron microscopy

Complexes between linear DNA and DnaA protein were formed in reaction volumes of 10 μl with 50 ng of DNA and variable amounts of protein as shown in the previous section for band-shift assays replacing bovine serum albumin from the binding with 5 mg/ml polyvinylpyrrolidone (PVP-K25; Fluka, Buchs, Switzerland) if band-shift assays were done in parallel. After incubation for 10 min at 37°C the complexes were fixed for 15 min in 0.2% glutaraldehyde at room temperature, diluted with the same volume of binding buffer and adsorbed to mica, positively stained in 2% uranyl acetate, rotary shadowed with Pt/Ir, and covered with a carbon film (Spiess and Lurz, 1988). Binding of DnaA protein to supercoiled plasmid DNA was done in a volume of 20 μl with 100 ng DNA and variable amounts of DnaA protein in binding buffer lacking BSA for 60 s at 37°C followed by fixation with 0.2% glutaraldehyde for 30 min on ice. After gel filtration with BioGelA5m (Bio-Rad Lab, Richmond, CA, USA) in buffer containing 10 mM HEPES–KOH, pH 7.5, 2.5 mM Mg-acetate, 0.5 mM EDTA, 2 mM DTE and 0.1% Triton X-100, the DNA was double-digested with *Pst*I and *Ssp*I. A second gel filtration followed in buffer without Triton and the complexes were prepared for electron microscopy by mica adsorption at 4°C. Micrographs were taken at a magnification of ×6700 in a Philips EM400T electron microscope on 35 mm film (RA711P, Agfa, Germany). The positions of the bound proteins were determined on 16× enlarged negatives using a LM4 digitizer (Brühl, Nürnberg, Germany). For each histogram the data of 150 to 300 DNA molecules showing DnaA complexes were evaluated using software developed in this laboratory (Perez-Martin *et al.*, 1989). In some experiments, nucleoprotein complexes were found at or very close to the ends of the fragments. This effect was reduced to background levels on blunt-ended fragments.

Apparently, DnaA bound to partially single-stranded ends; the resulting complexes were thus considered unspecific.

Acknowledgements

We gratefully acknowledge the skilful technical assistance of Gerhild Lüder and Michaela Welzeck. We thank Angelika Roth for the β-galactosidase::DnaA (domain 4) fusion protein, Olaf Kelm for the observation of trace topoisomerase I contaminations in our DnaA preparations, Margret Krause and Christian Speck for enjoyable discussions. This work was supported in part by grant SFB344/A9 of the Deutsche Forschungsgemeinschaft.

References

Baker,T.A., Funnell,B.E. and Kornberg,A. (1987) Helicase action of dnaB protein during replication from the *Escherichia coli* chromosomal origin *in vitro*. *J. Biol. Chem.*, **262**, 6877–6885.

Bates,D.B., Asai,T., Cao,Y., Chambers,M.W., Cadwell,G.W., Boye,E. and Kogoma,T. (1995) The DnaA box R4 in the minimal *oriC* is dispensable for initiation of *Escherichia coli* chromosome replication. *Nucleic Acids Res.*, **23**, 3119–3125.

Bramhill,D. and Kornberg,A. (1988) Duplex opening by dnaA protein at novel sequences in initiation of replication at the origin of the *E. coli* chromosome. *Cell*, **52**, 743–755.

Buhk,H.J. and Messer,W. (1983) Replication origin region of *Escherichia coli*: nucleotide sequence and functional units. *Gene*, **24**, 265–279.

Cassler,M.R., Grimwade,J.E. and Leonard,A.C. (1995) Cell cycle-specific changes in nucleoprotein complexes at a chromosomal replication origin. *EMBO J.*, **14**, 5833–5841.

Christensen,B.B. (1994) PhD thesis. Technical University of Denmark, Denmark.

Crooke,E., Thresher,R., Hwang,D.S., Griffith,J. and Kornberg,A. (1993) Replicatively active complexes of DnaA protein and the *Escherichia coli* chromosomal origin observed in the electron microscope. *J. Mol. Biol.*, **233**, 16–24.

Fuller,R.S., Kaguni,J.M. and Kornberg,A. (1981) Enzymatic replication of the origin of the *E. coli* chromosome. *Proc. Natl Acad. Sci. USA*, **78**, 7370–7374.

Fuller,R.S., Funnell,B.E. and Kornberg,A. (1984) The *dnaA* protein complex with the *E. coli* chromosomal origin (*oriC*) and other sites. *Cell*, **38**, 889–900.

Funnell,B.E., Baker,T.A. and Kornberg,A. (1987) *In vitro* assembly of a prepriming complex at the origin of the *Escherichia coli* chromosome. *J. Biol. Chem.*, **262**, 10327–10334.

Gille,H. and Messer,W. (1991) Localized unwinding and structural perturbations in the origin of replication, *oriC*, of *Escherichia coli in vitro* and *in vivo*. *EMBO J.*, **10**, 1579–1584.

Holz,A., Schaefer,C., Gille,H., Jueterbock,W.-R. and Messer,W. (1992) Mutations in the DnaA binding sites of the replication origin of *Escherichia coli*. *Mol. Gen. Genet.*, **233**, 81–88.

Hsu,J., Bramhill,D. and Thompson,C.M. (1994) Open complex formation by DnaA initiation protein at the *E. coli* chromosomal origin requires the 13-mers precisely spaced relative to the 9-mers. *Mol. Microbiol.*, **11**, 903–911.

Hwang,D.S. and Kornberg,A. (1992) Opening of the replication origin of *Escherichia coli* by DnaA protein with protein HU or IHF. *J. Biol. Chem.*, **267**, 23083–23086.

Kimura,T., Asai,T., Imai,M. and Takanami,M. (1989) Methylation strongly enhances DNA bending in the replication origin region of the *Escherichia coli* chromosome. *Mol. Gen. Genet.*, **219**, 69–74.

Kline,B.C., Kogoma,T., Tam,J.E. and Shields,M.S. (1986) Requirement of the *Escherichia coli dnaA* gene product for plasmid F maintenance. *J. Bacteriol.*, **168**, 440–443.

Kornberg,A. and Baker,T.A. (1992) *DNA Replication*. W.H. Freeman and Company, New York.

Langer,U., Richter,S., Roth,A., Weigel,C. and Messer,W. (1996) A comprehensive set of DnaA box mutations in the replication origin, *oriC*, of *Escherichia coli*. *Mol. Microbiol.*, **21**, 301–311.

Margulies,C. and Kaguni,J.M. (1996) Ordered and sequential binding of DnaA protein to *oriC*, the chromosomal origin of *Escherichia coli*. *J. Biol. Chem.*, **271**, 17035–17040.

Marszalek,J. and Kaguni,J.M. (1994) DnaA protein directs the binding of DnaB protein in initiation of DNA replication in *Escherichia coli*. *J. Biol. Chem.*, **269**, 4883–4890.

Matsui,M., Oka,A., Takanami,M., Yasuda,S. and Hirota,Y. (1985) Sites of *dnaA* protein-binding in the replication origin of the *E. coli* K-12 chromosome. *J. Mol. Biol.*, **184**, 529–533.

Messer,W. and Weigel,C. (1996) Initiation of chromosome replication. In Neidhardt,F.C., Curtiss,R.,III, Ingraham,J., Lin,E.C.C., Low,K.B., Magasanik,B., Reznikoff,W.S., Riley,M., Schaechter,M. and Umbarger,H.E. (eds), *Escherichia coli and Salmonella: Cellular and Molecular Biology*. ASM Press, Washington, DC, pp. 1579–1601.

Messer,W., Hartmann-Kühlein,H., Langer,U., Mahlow,E., Roth,A., Schaper,S., Urmoneit,B. and Woelker,B. (1992) The complex for replication initiation of *Escherichia coli*. *Chromosoma*, **102**, S1–S6.

Parada,C.A. and Marians,K.J. (1991) Mechanism of DNA A protein-dependent pBR322 DNA replication. DNA A protein-mediated *trans*-strand loading of the DNA B protein at the origin of pBR322 DNA. *J. Biol. Chem.*, **266**, 18895–18906.

Perez-Martin,J., Del Solar,G.H., Lurz,R., De la Campa,A.G., Dobrinski,B. and Espinosa,M. (1989) Induced bending of plasmid pLS1 by the plasmid-encoded protein RepA. *J. Biol. Chem.*, **264**, 21334–21339.

Roth,A. and Messer,W. (1995) The DNA binding domain of the initiator protein DnaA. *EMBO J.*, **14**, 2106–2111.

Samitt,C.E., Hansen,F.G., Miller,J.F. and Schaechter,M. (1989) *In vivo* studies of DnaA binding to the origin of replication of *Escherichia coli*. *EMBO J.*, **8**, 989–993.

Schaper,S. and Messer,W. (1995) Interaction of the initiator protein DnaA of *Escherichia coli* with its DNA target. *J. Biol. Chem.*, **270**, 17622–17626.

Sekimizu,K., Bramhill,D. and Kornberg,A. (1988a) Sequential early stages in the *in vitro* initiation of replication at the origin of the *Escherichia coli* chromosome. *J. Biol. Chem.*, **263**, 7124–7130.

Sekimizu,K., Yung,B.Y. and Kornberg,A. (1988b) The dnaA protein of *Escherichia coli*. Abundance, improved purification, and membrane binding. *J. Biol. Chem.*, **263**, 7136–7140.

Seufert,W. and Messer,W. (1987) Start sites for bidirectional *in vitro* replication inside the replication origin, *oriC*, of *Escherichia coli*. *EMBO J.*, **6**, 2469–2472.

Skarstad,K. and Boye,E. (1994) The initiator protein DnaA: evolution, properties and function. *Biochim. Biophys. Acta*, **1217**, 111–130.

Spiess,E. and Lurz,R. (1988) Electron microscopic analysis of nucleic acids and nucleic acid-protein complexes. *Methods Microbiol.*, **20**, 293–323.

Woelker,B. and Messer,W. (1993) The structure of the initiation complex at the replication origin, *oriC*, of *Escherichia coli*. *Nucleic Acids Res.*, **21**, 5025–5033.

Yoshikawa,H. and Ogasawara,N. (1991) Structure and function of DnaA and the DnaA-box in eubacteria: evolutionary relationships of bacterial replication origins. *Mol. Microbiol.*, **5**, 2589–2597.

Zakrzewska-Czerwinska,J. and Schrempf,H. (1992) Characterization of an autonomously replicating region from the *Streptomyces lividans* chromosome. *J. Bacteriol.*, **174**, 2688–2693.

Received on June 19, 1997; revised on July 29, 1997